ELSEVIER

Journal of Nuclear Materials 290–293 (2001) 628–632

journal of nuclear materials

www.elsevier.nl/locate/jnucmat

Effect of limiter recycling on measured poloidal impurity emission profiles in Tore Supra

J. Hogan [a,*], C. DeMichelis [b], P. Monier-Garbet [b], M. Becoulet [a], C. Bush [a], P. Ghendrih [b], R. Guirlet [b], W. Hess [b], M. Mattioli [b], J.C. Vallet [b]

[a] *Oak Ridge National Laboratory, Fusion Energy Division, Oak Ridge, TN 37830, USA*
[b] *CEA-Cadarache, St. Paul lez Durance, France*

Abstract

Poloidal impurity emission profiles measured with the Tore Supra grazing incidence duochromator exhibit a complex spatial structure during ergodic divertor operation with an outboard poloidal guard limiter. As previous measurements with inboard-wall limited plasmas have shown that these profiles give important information about the ergodic field structure, so the contribution of local neon recycling from the limiter-induced plume has been modeled. This permits a discrimination of edge and core transport effects. The BBQ 3D scrape-off layer code calculates the asymmetric contribution to the emission amd MIST 1D simulation gives the symmetric part. A systematic increase is observed in the decay rate of neon emission after injection as the ergodic divertor strength is increased. The calculations permit identification of the limiter plume contribution to the profile structure, and, with this identification, the effect of the divertor to enhance impurity efflux can be seen from the decay data. © 2001 Published by Elsevier Science B.V.

Keywords: Impurity transport; Tore Supra

1. Introduction

In addition to the fundamental importance of helium transport and exhaust, the detailed particle balance of recycling impurities such as neon, argon and krypton, which are used in advanced scenarios to ameliorate high heat fluxes in future reactors, is being explored on several machines. A workable advanced tokamak radiative scenario will require efficient impurity cleansing from the core, and an efficient use of extrinsically injected radiating impurities. The utility of advanced tokamak scenarios, such as internal transport barrier plasmas, may be limited by increased particle confinement, which has negative implications for helium exhaust in reactors [1]. The transition to improved confinement regimes encompasses both reduction in core transport and changes in scrape-off layer transport. Thus the delineation of the relative contributions of improved scrape-off layer screening versus reduced core diffusivity is an important issue.

As part of a Tore Supra campaign to prepare for strong radiation experiments, systematic poloidally resolved spatial profiles of neon impurity emission were obtained using a grazing incidence VUV duochromator [2]. The experiments were carried out in ohmic conditions, and were primarily intended to study screening of relatively small amounts of injected neon, not to optimize the radiation. For these preparatory experiments the Tore Supra low-field side ergodic divertor was used, at varying strength, and the outboard poloidal limiter was placed in advance of the divertor, to reduce divertor heat flux.

The conventional assumption in core impurity transport modeling is that the impurity sources at the edge enter as neutral impurities. In fact, especially on larger tokamaks, impurities are multiply ionized as they enter the core region, and they are distributed poloidally and toroidally. The presence of the guard limiter in these experiments, located relatively near to the duochromator, provides a potentially traceable local source of impurities in the scrape-off layer whose interaction with core transport can be studied.

* Corresponding author. Tel.: +1-865 574 1349; fax: +1-865 574 1191.
E-mail address: hoganjt@fed.ornl.gov (J. Hogan).

0022-3115/01/$ - see front matter © 2001 Published by Elsevier Science B.V.
PII: S0022-3115(00)00519-5

We first describe the physical layout of the duochromator and the space and time dependence of the profiles which were observed during a scan in ergodic divertor current. We then proceed to analyze the components of the complex duochromator profiles, describing the part due to symmetric emission from the core using the MIST radial impurity transport code and the asymmetric part, describing the scrape-off layer impurity ion source, with the BBQ scrape-off layer impurity transport code. The comparison of the model with the observed signal is then made. The comparison allows an interpretation of the components, and the discrimination of scrape-off layer and core components. The systematic variation of these components as the ergodic divertor current is scanned allows us to assess the impurity cleaning effects for the ergodic divertor.

2. Experimental conditions and duochromator data

The duochromator scans the plasma cross section poloidally, from the equator past the tangency radius of the emitting impurities Fig. 1(a). The outboard limiter, which was positioned 5 cm radially inward of the divertor radius for the experiments to be analyzed, is located in the same toroidal port as the duochromator, and is also situated on the outboard mid-plane Fig. 1(b).

With ergodic divertor operation the duochromator signal is complex, showing both the familiar, Abel-invertible annular peak near the tangency radius, where the chords intersect the plasma flux surface with the peak density of the ion in question, and a second significant peak near the equator. Fig. 2(a) shows the poloidal emissivity distributions for Ne IV, V, VII and VIII for fixed ergodic divertor current at fixed electron density ($\langle n_e \rangle = 2 \times 10^{19}$ m^{-3}, $I_{DE} = 45$ kA). The higher charge states have a larger equator peak, and the annular peak moves systematically inward, with fixed amplitude, for higher impurity charge, moving as expected toward regions of higher electron temperature. Fig. 2(b) shows the signal as the ergodic divertor current varies from zero to the maximum value of 45 kA. The strength of these peak signals also shows systematic variation. Elucidation of the behavior of the equator peak is one of the objectives of the simulation.

The duochromator signals have a slow decay after injection, due to residual background turbo-molecular pumping, and this can be used to provide impurity decay estimates ($\tau_{1/e}$). Fig. 3(a) shows the decay of the equator and tangency peak features for NeVII emission, with $\langle n_e \rangle = 3 \times 10^{19}$ m^{-3} and a variation in divertor current strength I_{DE} from 0 to 45 kA. The decay rate ($\tau_{1/e}^{-1}$) shows a systematic increase with I_{DE} for the equator component. The decay time $\tau_{1/e}$ increases from 4.7 s ($I_{DE} = 0$) to 3.4 s ($I_{DE} = 45$ kA). This suggests a ~40% increase of the total efflux of neon to the limiter under otherwise similar conditions. The tangency peak decay is similar for all values of I_{DE}. Fig. 3(b) shows the variation of the (possibly limiter-influenced) equator peak with ion

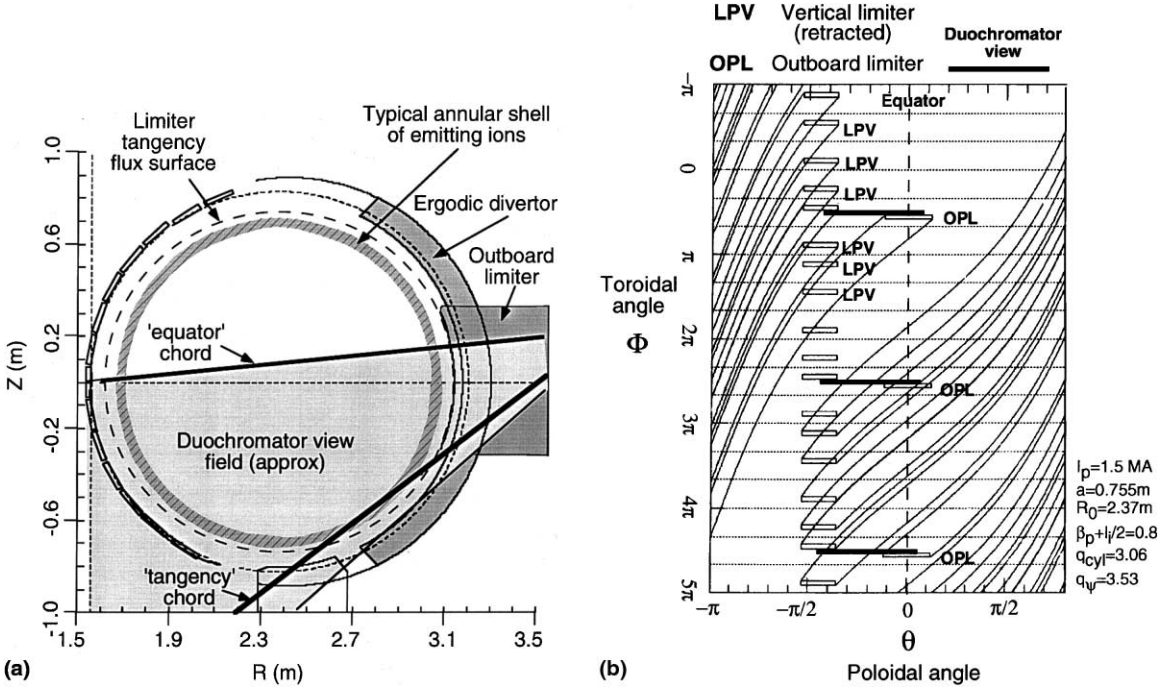

Fig. 1. (a) Poloidal geometry of the duochromator. (b) Toroidal geometry of the duochromator.

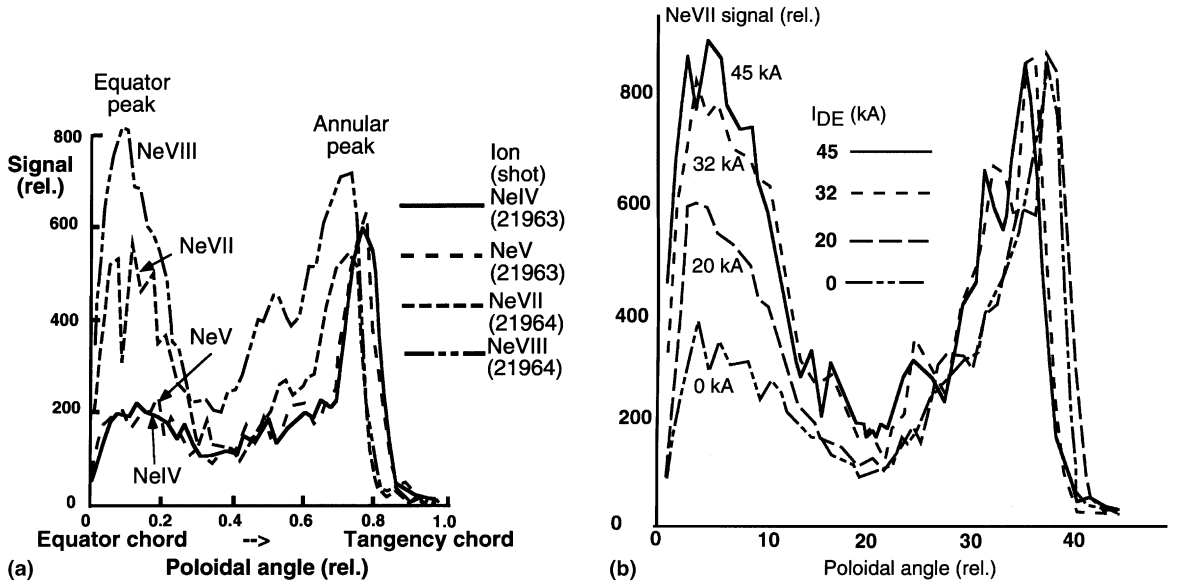

Fig. 2. Measured duochromator poloidal profiles: (a) dependence on ion charge with fixed divertor current; (b) variation of Ne VII emission profile with divertor current.

charge for fixed divertor current, showing here also a systematic increase in the efflux, this time for increasing ion charge. This would mean that the equator peak is a measure of the increased impurity efflux for more highly charged (thus hotter) ions in the periphery which can leave the plasma on the ergodized field lines. If this interpretation is correct, the duochromator signal is a charateristic of the limiter recycling source. Before this identification is possible, however, the origin of the equator peak has to be identified. We must separately consider the axi-symmetric and the asymmetric contributions to the measurement, then discuss the relative magnitudes of the components.

3. Scrape-off layer and core simulation

To simulate the poloidal impurity emission profiles, a combination of 1D radial, flux-surface averaged impurity transport with 3D scrape-off layer impurity transport has been used. The symmetric contribution is found by matching MIST [3] radial impurity transport calculations with data. The measured T_e and n_e radial and time-dependent profiles from Thomson scattering are used, and edge profiles (in the region $\rho > 0.86$ where Thomson measurements are not available) are estimated from ECE measurements of the variation of edge T_e with I_{DE} which have been made by Becoulet [4]. The MIST calculation was validated with a case in which relative charge-exchange recombination (CXS) profiles for both carbon and neon are available [5]. This allows the determination of the anomalous diffusivity and pinch velocity for the case with the strongest ergodic divertor current ($I_{DE} = 45$ kA). For this case, the MIST time-dependent analysis uses the anomalous diffusion coefficient $D_{Anom} = 0.335$ m^2/s for $\rho = 0.0$–0.75 and $D_{Anom} = 1$ m^2/s for $\rho > 0.75$, and an inward pinch velocity V_{Anom} which increases from 0 to 240 m/s for $0 < \rho < 0.75$ and is constant at $V_{Anom} = 240$ m/s for $\rho > 0.75$. The maximum values of D_{Anom} and V_{Anom} (reached at $\rho = 0.75$) are reduced linearly as the divertor current decreases. The MIST validation case compares the carbon and neon content from the CXS measurements with the absolute emission from the 33.4 A CVI Ly α line, the 40.27 A and 40.73 A CV R and I lines, the 18.97 A OVIII Ly α line, and the NeX 12.1 A Ly α line (seen in the second order); the absolute intensities of all these lines have been simultaneously measured by an extreme grazing incidence soft X-ray spectrometer. The carbon and oxygen contributions to the total radiation are matched before neon injection, and the incremental radiation due to neon injection is matched using radiation rates from the ADAS database.

Using these transport parameters, the core neon density evolution in discharges for an ergodic divertor current scan has been simulated using MIST to calculate, in parallel, the oxygen, carbon and neon space- and time-dependent evolution. The total radiation from each species is then added to match the observed level in these shots. The resulting neon emissivity measured by the duochromator is evaluated using photon emission coefficients recently calculated by Fournier et al. [6]. This gives the axially symmetric contribution to the duochromator signal.

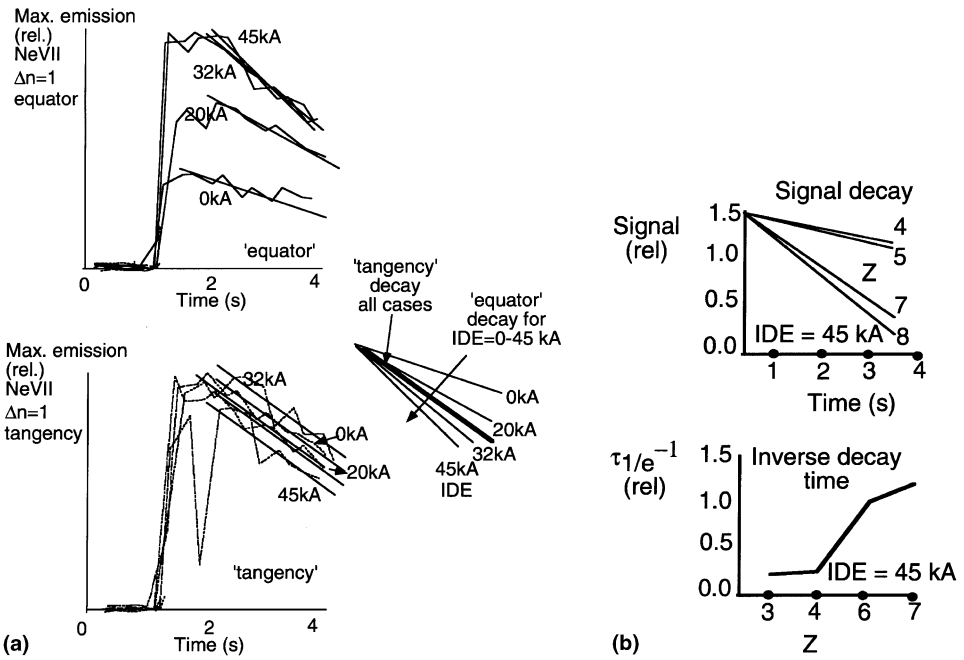

Fig. 3. Time decay of equator and tangency peaks: (a) with a scan in divertor current; (b) variation of the equator peak with ion charge at fixed divertor current (top), measured signal decay for different ion charge and (bottom) variation of the inferred 1/e decay time with ion charge.

The MIST calculations also use an improved boundary condition, in that impurity influxes are not treated as neutral carbon, oxygen and neon, but a distribution of ion charge states entering the core plasma is assumed. This distribution is found from 3D scrape-off layer calculations, which are described next. The BBQ SOL transport code [7,8] is used to calculate the poloidally and toroidally asymmetric contribution to the duochromator signal due to recycling. Starting from an assumed flux of recycled impurity neutrals, the scrape-off layer transport code follows the impurities as they are emitted from the limiter (with an energy distribution determined in part from TRIM reflection coefficients [9]) and undergo transport and ionization to higher charge states in the scrape-off layer. The particle tracking is stopped when they have penetrated 1 cm into the core plasma, and the resulting fluxes, charge distributions, and poloidal distributions are used as inputs to the MIST calculations. The asymmetric contributions to the emissivity for the neon ion charge states measured by the duochromator are calculated using the BBQ distribution of ion densities $n_Z^{(k)}(\rho,\theta,\phi)$ ($k=$ ion, $\rho=$ radius, $\theta=$ poloidal angle, $\phi=$ toroidal angle) to integrate over the duochromator sight lines, using the photon emission coefficients for the relevant line from [6].

Since both the MIST and the BBQ contributions to the signal are proportional to the same quantity (the recycling flux at the outboard limiter) the relative scale of the symmetric and asymmetric contribution to the duochromator signal is fixed.

4. Simulation of the duochromator signal

The asymmetric contribution due to neon recycling from the limiter is peaked at the equator, but the resulting contribution to the duochromator signal slightly shifted from the zero in poloidal angle because of the toroidal displacement of the duochromator with respect to the limiter and the resulting rotation of magnetic field lines. Fig. 4(a) and (b) shows the resulting match between the BBQ/MIST model and the data for T_e-dependent ($\Delta n=1$) lines of Ne VII and Ne VIII for shot 21982. The asymmetric component originates as neutral neon atoms recycling from the nearby limiter, and undergoing ionization and recombination as these atoms and ions stream into the view of the duochromator. The MIST/BBQ predicted composite signal for the relevant line is compared with the measured profile. The agreement is reasonable and allows the interpretation of the equator peak as due to recycling from the nearby limiter.

This comparison does not follow the detailed structure of the ergodic field in this region, and it is expected that detailed 'fine structure' in the poloidal profiles is an indicator of the ergodic field variation. This was found in the earlier case of inner wall-limited plasmas in Tore Supra [2] and will be the subject of future study.

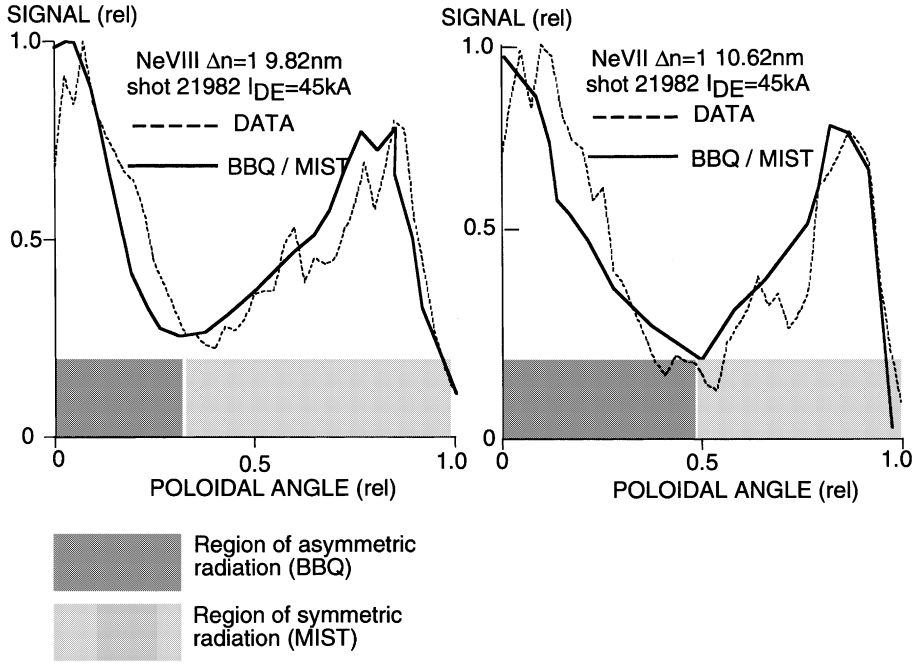

Fig. 4. Comparison of MIST/BBQ model with Ne VII and VIII signals for $I_{DE} = 45$ kA case.

5. Summary and conclusions

Previous study of poloidal impurity emission profiles for Tore Supra inner-wall limited (high-field side) plasmas with ergodic divertor has demonstrated the modulation of these profiles due to the imposed ergodic divertor field. Similar experiments with outboard-limiter (low-field side) configurations are more difficult to interpret because of the neay-by limiter. A detailed modeling study of the direct effect of the limiter plume, reflecting total impurity efflux from the core, has discriminated this effect from core related changes due to the divertor.

The use of the duochromator signals for impurity transport studies thus is justified since the edge recycling from the outboard limiter is shown to be a plausible source for the equator feature. The signal from the equator peak is thus indicative of the total efflux from the core plasma, and comparison with other core data should provide useful information about the relation between core and edge confinement. Thus, the systematic decreases seen in the duochromator decay times with increasing divertor current Fig. 3(a) can be interpreted as the response of the total impurity efflux. Similarly, the increase in the equator peak with increasing divertor current (Fig. 2(b)) is a reflection of the enhanced edge recycling caused by the ergodic layer. The core confinement, by contrast, is relatively unchanged as the divertor current is increased (Fig. 3(a)). Thus the ergodic layer may play a role similar to that of ELMs in axi-symmetric divertor experiments.

The MIST/BBQ model is thus able to provide both a qualitative and, in some cases, a quantitative prediction of the duochromator signal.

Acknowledgements

This research is sponsored in part by the US Department of Energy, under contract No. DE-AC05-00OR22725 with Oak Ridge National Laboratory managed by UT-Battelle, LLC.

References

[1] J. Hogan, D. Hillis, Nucl. Fus. 40 (879) 2000.
[2] C. DeMichelis et al., Plasma. Phys. Control Fus. 37 (95) 505.
[3] R. Hulse, Fusion Technol. 3 (1983) 259.
[4] M. Becoulet (private communication).
[5] W. Hess et al., EPS Budapest 2000, to appear.
[6] K. Fournier, M. Mattioli et al., Phys. Rev. E 60 (99) 4760.
[7] J. Hogan, C. Klepper, J. Harris et al., in: Proceedings of the 16th IAEA Conference on Plasma Physics and Control Fusion, Montreal, 1996.
[8] R. Giannella, Y. Corre, J. Hogan et al., in: Proceedings of the 26th European Conference On Control Fusion and Plasma Physics, Maastricht, Netherlands, 1999.
[9] W. Eckstein et al., IPP-Report 9/117, Garching, March 1998.